

# A non-PRE double-peaked burst from 4U 1636–536: evidence for burning front propagation

Sudip Bhattacharyya<sup>1,2</sup>, and Tod E. Strohmayer<sup>2</sup>

## ABSTRACT

We analyse Rossi X-ray Timing Explorer (RXTE) Proportional Counter Array (PCA) data of a double-peaked burst from the low mass X-ray binary (LMXB) 4U 1636–536 that shows no evidence for photospheric radius expansion (PRE). We find that the X-ray emitting area on the star increases with time as the burst progresses, even though the photosphere does not expand. We argue that this is a strong indication of thermonuclear flame spreading on the stellar surface during such bursts. We propose a model for such double-peaked bursts, based on thermonuclear flame spreading, that can qualitatively explain their essential features, as well as the rarity of these bursts.

*Subject headings:* accretion, accretion disks — relativity — stars: neutron — X-rays: binaries — X-rays: bursts — X-rays: individual (4U 1636–536)

## 1. Introduction

X-ray bursts are produced by thermonuclear burning of matter accumulated on the surfaces of accreting neutron stars (Grindlay et al. 1976; Belian, Conner, & Evans 1976; Woosley & Taam 1976, Joss 1977; Lamb & Lamb 1978). For most bursts, profiles are single peaked, with rise times of the order of a fraction of a second to a few seconds, and decay times of the order of ten or a few tens of seconds. However, for some bursts, double-peaked structure is observed. These peaks (with time separation of a few seconds) in a single luminous burst can normally be explained in terms of photospheric radius expansion (PRE; due to radiation pressure) and contraction (Paczynski 1983; Ebisuzaki, Hanawa, & Sugimoto 1984). As the photosphere expands, the effective temperature decreases, and the emitted photons shift towards lower energies. A subsequent contraction of the photosphere has the

---

<sup>1</sup>Department of Astronomy, University of Maryland at College Park, College Park, MD 20742-2421

<sup>2</sup>X-ray Astrophysics Lab, Exploration of the Universe Division, NASA’s Goddard Space Flight Center, Greenbelt, MD 20771; sudip@milkyway.gsfc.nasa.gov, stroh@clarence.gsfc.nasa.gov

opposite effect. This can cause a dip (and hence the double-peaked structure) in the high-energy burst profile (Lewin et al. 1976; Hoffman, Cominsky, & Lewin 1980), although such a structure is not frequently seen in bolometric or low-energy profiles (see Smale 2001).

Double-peaked structure in weak X-ray bursts was discovered by Sztajno et al. (1985) using EXOSAT observations of the low mass X-ray binary (LMXB) system 4U 1636–536. For these bursts, two peaks are seen in the bolometric profile, and even in low-energy profiles. For this reason, and as these bursts are not strong enough to cause photospheric expansion, some other physical effects are needed to explain them. Several models have been put forward to explain these non-PRE double-peaked bursts: (1) two-step energy generation due to shear instabilities in the fuel on the stellar surface (Fujimoto et al. 1988), (2) a nuclear waiting point impedance in the thermonuclear reaction flow (Fisker, Thielemann, & Wiescher 2004), (3) heat transport impedance in a two-zone model (Regev & Livio 1984), and (4) interactions with the accretion disk (Melia & Zylstra 1992). As we will elaborate in § 3, none of these models can explain various aspects of these bursts satisfactorily. In this Letter, we propose a model for the double-peaked bursts based on thermonuclear flame spreading on neutron stars, and comparing it qualitatively with the RXTE data of a double-peaked burst from 4U 1636–536, we show that our model can explain the essential features of these bursts.

## 2. Data Analysis and Model Calculations

We analyse the RXTE PCA archival data of a double-peaked burst (Date of observation: Jan 8, 2002; ObsId: 60032-01-19-000) from 4U 1636–536. The heights of the two peaks are almost identical ( $\sim 2200$  counts/s/PCU), with a dip depth more than half the peak height (Fig. 1). This is a weak burst compared to PRE bursts from this source, which can have  $\sim 7000$  counts/s/PCU (see Strohmayer et al. 1998). The burst profiles at different energy bands are very similar (Fig. 1), showing that this is not a PRE burst. However, the hardness in panel *b* of Fig. 1 shows two striking features: (1) the first peak of the hardness occurs 2–3 seconds before that of the burst profile; (2) the second hardness peak is much lower than the first one, while the burst profile peaks are of similar height. As the emitted flux primarily depends on source hardness (which is a measure of temperature) and source emission area, feature (1) indicates that the emission area increases with time. Feature (2) is possible if the emission area at the time of the second peak is much higher than that at the time of the first peak. As for a non-PRE burst, the emission area can increase only if the burning region spreads on the stellar surface from an initially small size, these two features are consistent with thermonuclear flame spreading (Strohmayer, Zhang, & Swank 1997; Kong et al. 2000).

As a next step, we break the burst profile into smaller time bins, and for each bin

perform spectral fitting. This gives the time evolution of the spectral parameters. We fit the data with a single temperature blackbody model (bbodyrad in XSPEC), as generally burst spectra are well fit by a blackbody (Strohmayer & Bildsten 2003). In doing this, we fix the hydrogen column density  $N_{\text{H}}$  at a value  $0.56 \times 10^{22} \text{ cm}^{-2}$  (van Paradijs et al. 1986). The results of these fits are shown in panels *c* & *d* of Fig. 1. The radius is calculated from the “normalization” and provides a measure of the source emitting area. The panels show that the evolution of the temperature is similar to that of the hardness (as expected), and the size of the emission area increases with time (indicating flame spreading), first quickly, and then more slowly. The temporal behavior of the radius also shows that this is not a PRE burst, otherwise the radius would decrease from the time when the burst profile attains its minimum between the two peaks. However, the reduced  $\chi^2$  values are high for these fits ( $> 1.5$  for 13 out of 29 time bins). Considering the arguments of the previous paragraph, this may be because of the following reason: the emission is locally blackbody, but temperatures at different locations on the stellar surface are significantly different (as a result of slow flame spreading in comparison to the timescale of temperature decay at a given location), and hence a single temperature blackbody model can not fit the observed spectra well. However, the similar evolution of temperature to that of the hardness indicates that these fits give average blackbody temperatures on the stellar surface. This explains the smaller height of the second temperature peak (panel *c*, Fig. 1), as with the slow flame spreading, temperature decays on most part of the star before the flame engulfs the whole star, making the average temperature smaller during the second peak. The error bars in panels *c* & *d* of Fig. 1 give  $1\sigma$  errors. As the reduced  $\chi^2$  values for some of the time bins are high, increasing  $\chi^2$  by 1 from the best fit value would underestimate these errors. Therefore, we increase  $\chi^2$  by the amount of the reduced  $\chi^2$  of the fit to calculate the  $1\sigma$  errors.

From the above analysis we infer that double-peaked bursts may be caused by thermonuclear flame spreading on the stellar surface. In order to show this, in our simple model, we consider that the fuel (accreted matter) is distributed over the entire stellar surface, the burst is ignited at a certain point, and then propagates on the surface to ignite all the fuel gradually. For the particular double-peaked burst analysed here, we assume that the burning region forms a  $\phi$ -symmetric belt very quickly after ignition at or near the north pole (while the observer’s inclination angle, measured from this pole, is  $\leq 90^\circ$ ), in order to explain the non-observation of millisecond period brightness oscillations, and the initially fast moving front “stalls” for a time as it approaches the equator, before speeding up again into the opposite hemisphere. This causes the burning front to take more time to reach the equator from the mid-latitudes, and during that time hot portions of the star can cool, causing a decrease in the emitted flux. Approaching the equator, the front propagation speed increases again, causing an increase of the emitted flux and the observed double-peaked structure.

To qualitatively test this hypothesis we calculate the corresponding model, assuming that the emitting region is a  $\phi$ -symmetric belt extending from the north pole to a polar angle  $\theta_{\text{edge}}$ . To compare this model with the data, we need to calculate the flux and spectrum at a certain time elapsed since burst onset ( $\Delta t$ ), and hence it is essential to know  $\theta_{\text{edge}}$  and the temperature at a given  $\theta$ -position in the belt as functions of  $\Delta t$ . The first one can be determined from  $\Delta t = \int_0^{\theta_{\text{edge}}} d\theta / \dot{\theta}(\theta)$ , if the burning front speed  $\dot{\theta}(\theta)$  is known. To calculate the temperature, we assume that after ignition the temperature increases from  $T_{\text{low}}$  to  $(T_{\text{low}} + (0.99 \times (T_{\text{high}} - T_{\text{low}})))$  following the equation  $T(t) = T_{\text{low}} + (T_{\text{high}} - T_{\text{low}}) \times (1 - \exp(-t/t_{\text{rise}}))$ , and then decays exponentially with an e-folding time  $t_{\text{decay}}$ . In our model, we assume that  $\dot{\theta}(\theta) = F(\theta) = 1/(t_{\text{total}} \times \cos \theta)$  for  $\theta \leq 90^\circ$ , and  $\dot{\theta}(\theta) = F(180^\circ - \theta)$  for  $\theta \geq 90^\circ$ , where  $t_{\text{total}}$  is the time needed by the front to propagate from a pole to the equator in the absence of any stalling. This expression of  $\dot{\theta}(\theta)$  follows from Spitkovsky et al. (2002), as the neutron star in 4U 1636–536 is rapidly rotating (spin frequency  $\nu_* \approx 582$  Hz; Giles et al. 2002; Strohmayer & Markwardt 2002), and hence the effect of the Coriolis force on the flame speed should be important. We assume that the stalling of the front happens between the polar angles  $\theta_1$  and  $\theta_2$  in the northern hemisphere:  $\dot{\theta}(\theta)$  decreases linearly from  $\theta = \theta_1$  to  $\theta = \theta_m$ , reaching a value  $s/t_{\text{total}}$ , and then increases linearly up to  $\theta = \theta_2$  reaching a value  $F(\theta_2)$ . In our calculations, we consider the Doppler, special relativistic, and general relativistic (gravitational redshift and light-bending in Schwarzschild spacetime) effects. We compute model lightcurves and spectra for a range of parameter values, and show an example in Fig. 2, which qualitatively reproduces the observed features of the double-peaked burst. In panel *a* of Fig. 2, the burst profiles qualitatively match (including the depth of the dip) the data (see Fig. 1), except the initial rise. For the model, the initial rise time is longer than that for the data. An effect which may account for this discrepancy is the radiative diffusion time, ie. the delay between ignition at depth and emergence of the radiation. Note also that we calculate the model flux only up to the time when the burning front reaches the south pole, while in Fig. 1, the real data probably extend beyond that time. In panels *b* and *c* of Fig. 2, we plot the model hardness and average temperature on the stellar surface, respectively. We also fit our normalised model spectra with the XSPEC model `bbbodyrad`, in the same manner as for the data. The resulting blackbody temperature and radius are shown in panels *d* and *e* of Fig. 2. Panels *b*, *c* and *d* show a similar temporal behavior: both hardness and temperature increase at the beginning rapidly, then decrease up to the point when the burst profile reaches a minimum, increase slightly up to the point when the burst profile reaches the second peak, and then decrease again. This behavior is strikingly similar to that seen in the burst data (Fig. 1). We note that the temporal behavior of the model average temperature (Fig. 2) suggests that spectral fitting with a single temperature blackbody model actually does give the average temperature on the stellar surface. In panel *e* of Fig. 2, the evolution of the radius shows an initial rapid increase, and then a slower increase, which is also quite similar

to the data (Fig. 1). Therefore, simple modeling of pole to pole flame spreading (with a temporary stalling) can reproduce the essential features of this double-peaked burst.

We note that the burst lightcurves are sensitive to the values of the parameters, such as  $\theta_1$ ,  $\theta_2$ ,  $\theta_m$ , etc. quantitatively, but not qualitatively. For example, the main effects of the increase of  $\theta_1$ ,  $\theta_2$ ,  $\theta_m$ ,  $s$ ,  $t_{\text{total}}$ ,  $t_{\text{rise}}$  and  $t_{\text{decay}}$  are to decrease  $d$ , slightly decrease  $d$ , decrease  $p$ , decrease  $l$ , increase the timescale of the whole burst, increase the rise time of the second peak, and decrease  $l$  respectively. Here,  $d$  is the time separation between the two peaks relative to the burst duration,  $p$  is the ratio of the flux of second peak to that of first peak, and  $l$  is the ratio of the depth of the dip (from the second peak) to the second peak height.

### 3. Discussion and Conclusions

In this Letter we have presented a new model for double-peaked bursts, that naturally explains the observed increase in emission area, which other models do not. Moreover, it appears unlikely that model 1 (see § 1) can reproduce both the burst profile and the evolution of hardness (or, temperature) simultaneously, as it does not consider the emission area increase. There is also no real calculation of double-peaked profiles from this model. In addition, if thermonuclear flames spread in the way Spitkovsky et al. (2002) argue, it is very difficult to see how sufficient unburnt fuel (as required by model 1) can be maintained on top of the burnt fuel, as the full scale height of the hot fuel is likely overturned and mixed with the cold fuel. We suggest that models 2 & 3 (see § 1) are probably unable to reproduce the large dip (judging from the figures of Regev & Livio 1984; Fisker, Thielemann, & Wiescher 2004), seen in the observed burst. It is also unclear whether these models, as well as model 4 (see § 1), can explain the observed hardness and/or temperature evolution, and the rarity of the double-peaked bursts. Note that the naive interpretation of a double-peaked burst as two subsequent bursts (possibly in two hemispheres) can be ruled out, because these two bursts would have to be localized (probably by two magnetic poles; otherwise flame spreading without stalling would give rise to a single peak), and in that case we would expect to observe millisecond period brightness oscillations. Our model can qualitatively reproduce the essential features of the double-peaked bursts (see § 2), including the burst profile (with a large dip) and the hardness evolution. However it requires the burning front to stall for a few seconds, which clearly warrants some justification and further study. We suggest that accretion may provide a mechanism to slow the front, although a detailed theoretical calculation and modeling of the data are required to establish this. The magnetic field of the neutron star in 4U 1636-53 is probably comparatively low (as the source is not a millisecond X-ray pulsar), and accretion likely proceeds via a disk around the equatorial

plane. Therefore, a weak burst ignited near the north pole and proceeding towards the equator may be impeded and stalled by the pole-ward flow of accreted matter in the mid-latitudes, as this matter spreads from the equator towards the poles, first rapidly, then more slowly (Inogamov & Sunyaev 1999). After reaching the vicinity of the equator, the burning region may be able to inhibit accretion sufficiently to allow the front to speed up again. This is because the gravitational force on particles falling onto the star via a disk is closely balanced by the centrifugal force, and hence even weak bursts can probably inhibit accretion (see Inogamov & Sunyaev 1999), if thermonuclear flux is radiated near the equator. The cessation of accretion may also allow the observer to get X-ray flux from the burning region in some parts of the southern hemisphere. We emphasize that the credibility of these arguments depends on the justification of accretion induced impedance of front propagation, as the accretion flows exist much above the burning layer. Here we give the following qualitative arguments. The  $\phi$  component of linear speed ( $v_\phi$ ) of accreted matter in the stellar atmosphere (in mid-latitudes and near the equator) is  $\sim 10^5$  km s $^{-1}$  (Fujimoto et al. 1988), and the corresponding latitudinal ( $\theta$ ) component ( $v_\theta$ ) may be  $\sim 1000$  km s $^{-1}$  (Inogamov & Sunyaev 1999). Such accreted matter is likely to produce differential rotation in the inner layers by the inflow of the angular momentum, which may extend down through the burning shell (at the column depth of  $\sim 10^8$  gm cm $^{-2}$ ; Fujimoto et al. 1988). Therefore, in the burning layer,  $v_\theta$  may be comparable to the flame speed, which may be  $\leq 10$  km s $^{-1}$  for a rapidly spinning star ( $g \sim 10^{14}$  cm s $^{-2}$ ,  $f = 3657$  rad s $^{-1}$  at  $\theta = 60^\circ$ ; Spitkovsky et al. 2002). As a result, the burning front could plausibly be influenced by the accretion-induced pole-ward motion of burning shell matter.

Double-peaked structure appears only to be associated with weak bursts, perhaps because strong bursts would tend to disrupt accretion sufficiently to preclude the kind of front stalling that is required for the occurrence of two peaks according to our model. The double-peaked feature is somewhat rare even among the weak bursts. This may be because in order to have the double-peaked structure, the burst needs to be ignited at or near a pole (so that the accretion can continue for a few seconds), which is less probable than equatorial ignition (Spitkovsky et al. 2002). The fact that double-peaked bursts are seen from only a few sources (mostly from 4U 1636–536) can be understood in our model as follows. These bursts require a low stellar magnetic field (for a given accretion rate), so that accretion happens mostly through a disk in the equatorial plane, and the disk must closely approach the star (so that the gravitational force is closely balanced by the centrifugal force near the surface). This is possible, if the stellar equatorial dimensionless radius to mass ratio  $R/M$  is large, and  $\nu_*$  is high (making the radius of the innermost stable circular orbit small; Bhattacharyya et al. 2000). This relatively fine tuning among magnetic field, accretion rate, equatorial  $R/M$  and  $\nu_*$  may exist for a relatively small fraction of LMXBs. Therefore, our model qualita-

tively explains the enigmatic rarity of the non-PRE double-peaked bursts, and may also, in principle, enable constraints on stellar magnetic fields and equatorial  $R/M$  to be obtained.

Our work suggests that non-PRE double-peaked bursts can be important in understanding thermonuclear flame spreading on neutron stars, which may provide important insights about the millisecond period brightness oscillations during X-ray bursts, and hence can be useful for constraining equation of state models of the dense matter in the cores of neutron stars (Bhattacharyya & Strohmayer 2005; Bhattacharyya et al. 2005). However, the rarity of such bursts has been an obstacle to understanding them, and thus new attempts to expand the sample of these bursts seems well warranted.

This work was supported in part by NASA Guest Investigator grants.

## REFERENCES

- Belian, R. D., Conner, J. P., & Evans, W. D. 1976, *ApJ*, 206, L135.
- Bhattacharyya, S., & Strohmayer, T. E. 2005, *ApJ*, 634, L157 (astro-ph/0509370).
- Bhattacharyya, S., Strohmayer, T. E., Miller, M. C., & Markwardt, C. B. 2005, *ApJ*, 619, 483.
- Bhattacharyya, S., Thampan, A. V., Misra, R., & Datta, B. 2000, *ApJ*, 542, 473.
- Ebisuzaki, T., Hanawa, T., & Sugimoto, D. 1984, *PASJ*, 36, 551.
- Fisker, J. L., Thielemann, F., & Wiescher, M. 2004, *ApJ*, 608, L61.
- Fujimoto, M. Y., Sztajno, M., Lewin, W. H. G., & van Paradijs, J. 1988, *A&A*, 199, L9.
- Giles, A. B., Hill, K. M., Strohmayer, T. E., & Cummings, N. 2002, *ApJ*, 568, 279.
- Grindlay, J. E. et al. 1976, *ApJ*, 205, L127.
- Hoffman, J. A., Cominski, L. R., & Lewin, W. H. G. 1980, *ApJ*, 240, L27.
- Inogamov, N. A., & Sunyaev, R. A. 1999, *Astronomy Letters*, 25, 269.
- Joss, P. C. 1977, *Nature*, 270, 310.
- Kong, A. K. H., Homer, L., Kuulkers, E., Charles, P. A., & Smale, A. P. 2000, *MNRAS*, 311, 405.
- Lamb, D. Q., & Lamb, F. K. 1978, *ApJ*, 220, 291.
- Lewin et al. 1976, *MNRAS*, 177, 83P.
- Melia, F., & Zylstra, G. J. 1992, *ApJ*, 398, L53.
- Paczynski, B. 1983, *ApJ*, 276, 315.
- Regev, O., & Livio, M. 1984, *A&A*, 134, 123.
- Smale, A. P. 2001, *ApJ*, 562, 957.
- Spitkovsky, A., Levin, Y., & Ushomirsky, G. 2002, *ApJ*, 566, 1018.
- Sztajno, M. et al. 1985, *ApJ*, 299, 487.



Strohmayer, T. E., & Bildsten, L. 2003, in *Compact Stellar X-ray Sources*, Eds. W.H.G. Lewin and M. van der Klis, (Cambridge University Press: Cambridge), (astro-ph/0301544).

Strohmayer, T. E., & Markwardt, C. B. 2002, *ApJ*, 577, 337.

Strohmayer, T. E., Zhang, W., & Swank, J. H. 1997, *ApJ*, 487, L77.

Strohmayer, T. E., Zhang, W., Swank, J. H., White, N. E., & Lapidus, I. 1998, *ApJ*, 498, L135.

van Paradijs, J. et al. 1986, *MNRAS*, 221, 617.

Woosley, S. E., & Taam, R. E. 1976, *Nature*, 263, 101.

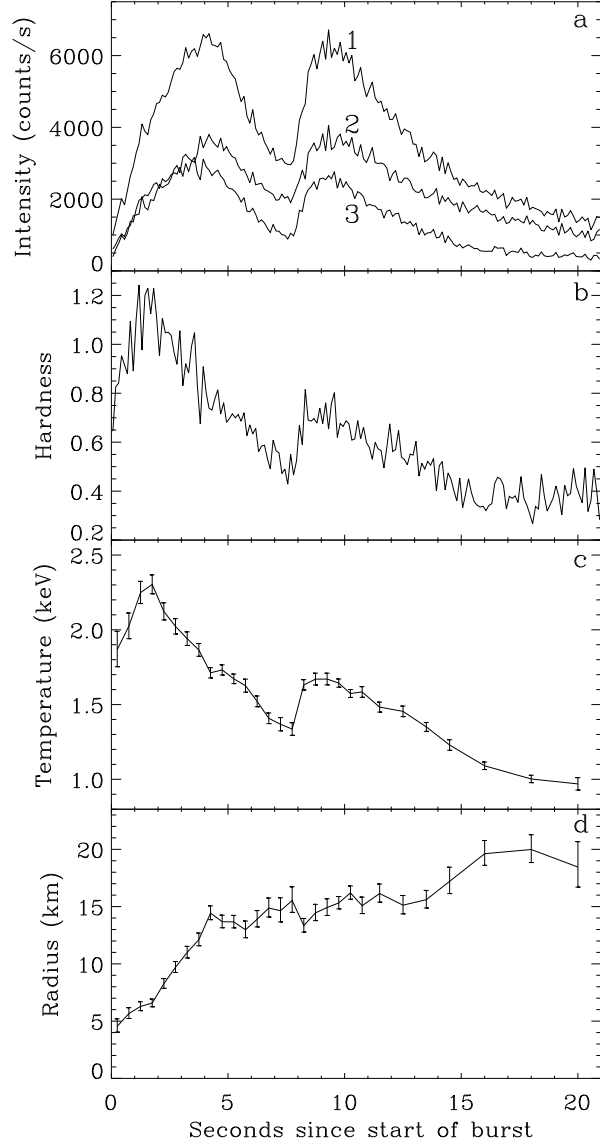


Fig. 1.— Double-peaked burst from 4U 1636–536: panel *a* gives the burst profiles (for 3 PCUs on): curve 1 is for the channel range 0 – 63 (nearly bolometric), curve 2 is for the channel range 0 – 10 (energy < 6.52 keV), and curve 3 is for channel range 11 – 63 (energy > 6.52 keV). Panel *b* shows the time evolution of hardness (ratio of counts in 11 – 63 channel range to that in 0–10 channel range). For both these panels, the size of the time bin is 0.125 s. Panels *c* & *d* show the time evolution of the blackbody temperature and the apparent radius (assuming 10 kpc source distance) of the emission area respectively, obtained by fitting the burst spectrum (persistent emission subtracted) with a single temperature blackbody model.

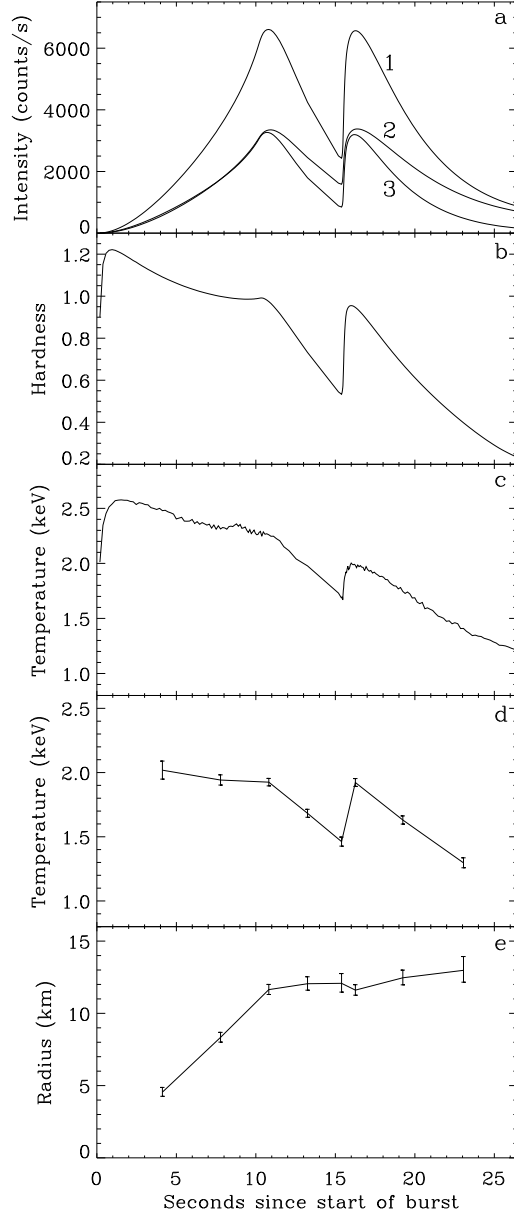


Fig. 2.— Model (convolved with a PCA response matrix) of double-peaked bursts: for all the panels, the burst is normalised so that its first intensity peak has the same count rate as that of the first peak of the observed burst. Panels *a* & *b* are similar to those of Fig. 1. Panel *c* gives the time evolution of average blackbody temperature on the stellar surface. Panels *d* & *e* are similar to panels *c* & *d* of Fig. 1 respectively. For these two panels, spectra are calculated for 0.5 s time bins for each point. Model parameter values are the following: stellar mass  $M = 1.5M_{\odot}$ , dimensionless stellar radius to mass ratio  $R/M = 5.5$ , stellar spin frequency  $\nu_* = 582$  Hz, observer’s inclination angle (measured from north pole)  $i = 50^{\circ}$ ,  $\theta_1 = 67^{\circ}$ ,  $\theta_m = 83^{\circ}$ ,  $\theta_2 = 87^{\circ}$ ,  $s = 0.04$ ,  $t_{\text{total}} = 11$  s,  $t_{\text{rise}} = 0.05$  s,  $t_{\text{decay}} = 6$  s,  $T_{\text{low}} = 1$  keV, and  $T_{\text{high}} = 2.8$  keV (see text for the definitions of the parameters).